

Analysis of the Effect of Steam-to-Biomass Ratio in Fluidized Bed Gasification with Multiphase Particle-in-cell CFD Simulation

Janitha C. Bandara¹ Marianne S. Eikeland¹ Britt M. E. Moldestad¹

¹Faculty of Technology, Natural Sciences and Maritime Sciences, University College of Southeast Norway
{Janitha.bandara, Marianne.Eikeland, britt.moldestad}@usn.no

Abstract

Biomass has been identified as a key renewable energy source to cope with upcoming environmental challenges. Gasification of biomass is becoming interested in large scale operation, especially in synthesis of liquid fuels. Bubbling and circulating fluidized bed gasification technology has overrun the interest over fixed bed systems. CFD studies of such reactor systems have become realistic and reliable with the modern computer power. Gasifying agent, temperature and steam or air to biomass ratio are the key parameters, which are responsible for the synthesis gas composition. Therefore, multiphase particle-in-cell CFD modeling was used in this study to analyze the steam to biomass, S/B, ratio in fluidized bed gasification.

Due to the complexity of the full loop simulation of dual circulating fluidized bed reactor system, only the gasification reactor was considered in this study. Predicted boundary conditions were implemented for the particle flow from the combustion reactor. The fluidization model was validated against experimental data in beforehand where Wen-Yu-Ergun drag model was found to be the best. The effect of the S/B ratio was analyzed at a constant steam temperature of 1073K and a steam velocity of 0.47 m/s. Four different S/B of 0.45, 0.38, 0.28 and 0.20 were analyzed. The biomass was considered to be in complete dry condition where single step pyrolysis reaction kinetics was used. Each gasification simulation was carried out for 100 seconds. 8% reduction of hydrogen content from 57% to 49% and 17% increment of carbon monoxide from 13% to 30% were observed when the S/B was reduced from 0.45 to 0.20. Countable amounts of methane were observed at S/B of 0.28 and 0.20. The lower heating value of the product gas increased from 10.1 MJ/kg to 12.37 MJ/kg and the cold gas efficiency decreased from 73.2% to 64.6% when the S/B was changed from 0.45 to 0.20. The specific gas production rate varied between 1.64 and 1.04 Nm³/kg of biomass.

Keywords: Biomass gasification, fluidized beds, gasifying agent, multiphase particle-in-cell

1 Introduction

Biomass was one of the key energy sources until the invention of cheap refined petroleum fuels in the 1940s. Since then, biomass energy technologies were not impressively developed until the oil crisis in the 1970s. Since then, biomass-to-energy conversion technologies were subjected to enormous research and developments. Biomass is further outdoing among other renewable energy systems, as it demands to be the sole alternative to replace all use of fossil fuels (Demirbas 2008). Bioenergy is also a key component in setting up the EU energy target of 20-20-20¹ where 10% of the transport related energy is supposed to be achieved via renewables (Scarlat, Dallemand et al. 2011).

Approximately 125 billion liters of biofuels were produced in 2015 where 75% is bio-ethanol and 25% is bio-diesel (Century 2015). The main feedstocks for bio-ethanol have been sugarcane and corn. However, there has been a long term debate of utilizing food commodities for energy production (Naik, Goud et al. 2010). On the other hand, annual terrestrial biomass production by green plants is approximately 100 billion tons of dry organic matter where only a 1.25% is derived as food (Naik, Goud et al. 2010). In other words, 90% of the world accessible biomass stocks are lignocellulosic (Szczodrak and Fiedurek 1996). Therefore, liquid biofuels from lignocellulosic materials, referred as second-generation biofuels, will provide more aspects to the future transportation industry.

Combustion, pyrolysis and gasification are the three main thermo-chemical technologies for conversion of biomass to energy, which eliminate most of the drawbacks related to bio-chemical conversion. Gasification converts solid biomass into a gaseous mixture of carbon monoxide (CO), hydrogen (H₂), methane (CH₄), carbon dioxide (CO₂) and minor fractions of higher molecular hydrocarbons such as tars. The product gas, which is referred as synthesis gas, could be processed into biofuels either by biological fermentation or Fisher-Tropsch (Munasinghe and Khanal 2010). In contrast, the producer gas could be directly combusted in furnaces, boilers, turbines and IC engines or used in solid oxide fuel cells.

¹ 20% reduction of CO₂ emissions, 20% increase of energy efficiency and 20% renewable energy share by 2020

Carbon to Hydrogen (C:H) ratio is the most important parameter in downstream processing of synthesis gas into liquid fuels. It is therefore important to optimize both the syngas composition and flowrates. In this picture, steam is much more desired as the gasification agent compared to air. Steam is further useful in tar cracking via reforming reactions as well. Dual circulating fluidized bed (DCFB) gasification is the best technology, compared to fixed bed and single bubbling fluidized bed reactor, to achieve a high H₂ content in synthesis gas.

This particular DCFB system separates the gasification and combustion reactions into two reactors as illustrated in Figure 1. Drying, pyrolysis and gasification (gas reactions and part of the char reduction) reactions are carried out in the gasification reactor, which normally operates with steam in the bubbling fluidization regime. Temperature and steam-to-biomass ratio (S/B) are the most important parameters for the gas composition. The remaining char from the gasifier is oxidized in the combustion chamber, which provides the heat demand of the gasification via circulation of bed material. Computational fluid dynamic (CFD) simulations integrated with reactions are more convenient, cost effective and efficient in optimization compared to experimental investigations.

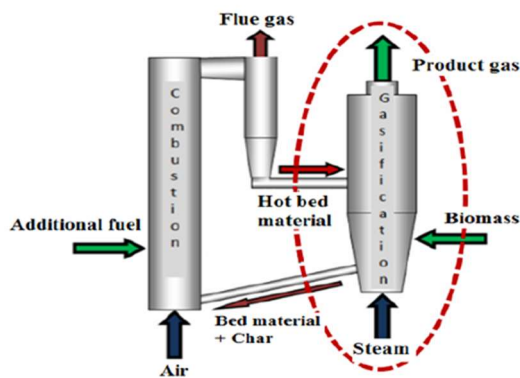


Figure 1. Dual circulating fluidized bed reactor

However, CFD modeling of particle systems are rather complex, and fluidized bed gasification is especially challenging due to the introduction of heterogeneous reactions together with heat and mass transfer. Eulerian-Eulerian (EE) and Eulerian-Lagrangian (EL) are the two basic approaches in modeling particle systems. The multiphase particle-in-cell (MP PIC) technique is an extended version of EL modeling which overcome certain limitations of conventional EL simulations such as modeling of dense particle systems with a large number of particles.

In the MP-PIC approach, the fluid phase is modeled in the Eulerian grid with Navier Stokes equations. Particles having similar characteristics such as size, density, etc. are parceled into units, which are referred as computational particles. Hence, billions of particles could be encapsulated into millions of computational

particles and modelled in the Lagrangian frame of reference (Andrews and O'Rourke 1996). Inter particle stresses are calculated in the Eulerian grid considering the particles as a continuum phase and those values are mapped back to the individual particles, using interpolation functions (Snider 2001). It has found that the required quantity of parcels to model the particle phase accurately is acceptable which realizes the simulation of large-scale particle systems.

The Barracuda VR commercial package is specially developed for multiphase CFD simulations, which uses the MP-PIC approach. This novel approach is referred to as computational particle fluid dynamics (CPFD). Solnordal, Kenche et al. 2015 and Liang, Zhang et al. 2014 have carried out MP PIC simulations for bubbling fluidized beds. Snider, Clark et al. 2011 has presented the integration of heat and reaction chemistry in MP PIC simulations whereas Loha, Chattopadhyay et al. 2014 and Xie et al Xie, Zhong et al. 2012 have carried out gasification simulations in a bubbling fluidized bed reactor. Liu, Cattolica et al. 2015, and Liu, Cattolica et al. 2016 have performed MP PIC simulations in a complete circulating dual fluidized bed system. The ability of defining multi-component particles is a distinctive feature of Barracuda, and facilitates the integration of volatization reactions involved in gasification and combustion.

A complete loop CFD simulation of the circulating fluidized bed gasification is complex in terms of generating the computational grid and expensive regarding simulation time. On the other hand, the underlying objective of this work is to analyze the effect of S/B in the gasification reactor. Hence, the CFD simulation was narrowed down to the gasification reactor as highlighted in Figure 1.

2 Barracuda CFD setup

The fluidization model was validated with cold bed fluidization experiments and the data has been published by the same author (Bandara, Thapa et al. 2016).

A simple cylindrical geometry of 2000 mm in height and 550 mm in diameter was used. The uniform grid option was applied with 4840 cells in total. The computational grid, boundary conditions and filling of the initial particle species in the bed are illustrated in Figure 2 where other operational and physical parameters are tabulated in Table 1. Uniform steam distribution was used while the steam velocity was maintained slightly above the minimum fluidization velocity. The hot bed material inlet was set as it guides the particle trajectory into the center of the reactor. Particle should driven into the system with a fluid flow where the fluid volume can be manipulated with “slip velocity” option. The bed material outflow was adjusted by changing the pressure at that particular cell where it was connected to the bed material inflow with “particle feed control” option.

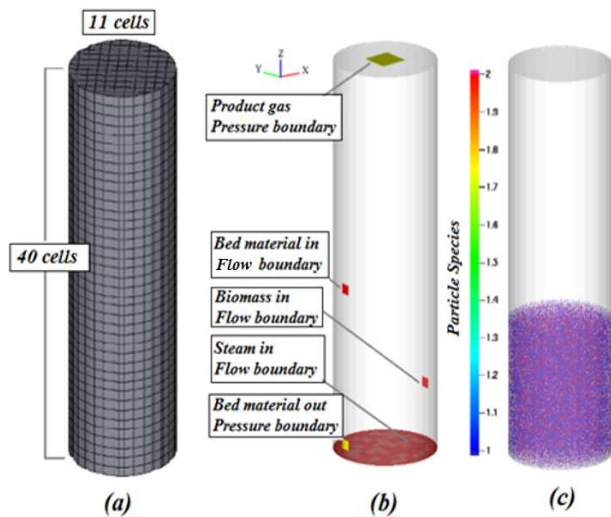


Figure 2. (a) Computational grid, (b) boundary conditions, (c) initial particle species

Table 1. Initial and boundary conditions

Flow boundary parameters			
Stream	Boundary	Parameters	Particle
Steam	Flow	1073 K, 101325 pa, 0.47 m/s	Nil
Gas out	Pressure	101325 pa	Nil
Biomass in	Flow	400 K, 101325 pa, 0.5 m/s,	0.05 kg/s
Bed Material in	Flow	1273 K, 101325 pa, 0.25 m/s	95% of bed material out
Bed Material out	pressure	101325 pa	Particle out flow
Initial conditions			
Fluid	1073 K, 101325 pa, steam, total volume		
Silica	1073 K, 101325 pa, 1000 μm , spherical, 0.48 volume fraction, density 2200 kg/m ³ , 600 mm height initial fill		
Char	1073 K, 101325 pa, 500 μm , spherical, 0.12 volume fraction, density 300 kg/m ³ , 600 mm height initial fill		

Steam pressure and the temperature of the incoming bed material were kept constant throughout all the simulations. It was intended to keep the fluidization behavior and residence time as similar as possible for all the simulations. Therefore, the steam flow boundary was maintained at 0.47 m/s. The S/B ratio was adjusted by changing the biomass flow. Four different S/B ratios of 0.45, 0.38, 0.28 and 0.2, were considered. As particle heating consumes high simulation time, initial particle temperature was set up same as that of the steam. It was further assumed that the initial bed composed with a fraction of char as well.

The Arrhenius reaction rates were used in the homogeneous and heterogeneous reactions. The constants in the reaction models were adapted from Thapa et al (R.K. Thapa, C. Pfeifer et al. 2014) and are tabulated in Table 2. The pyrolysis was modelled as a single step reaction, where the rate is given by,

$$264000 m_s \theta_f \exp \left[\frac{-1262}{T} \right] \quad (1)$$

Following the literature data, the composition of biomass was assumed to be 25% char and 75% volatiles

with no moisture and ash. Formation of tar and higher molecular hydrocarbons was neglected, and only H₂, CO, CO₂, CH₄ and H₂O were considered. Weight fractions of CH₄, CO, CO₂ and H₂ in the pyrolysis gas were taken as 0.1213, 0.6856, 0.1764 and 0.0167 respectively (R.K. Thapa, C. Pfeifer et al. 2014). Simulations were carried out for 100s and the gas composition, gas temperature and particle mass flow rates were analyzed.

Table 2. Reaction kinetics

Steam Reforming $C + H_2O \leftrightarrow H_2 + CO$	Forward	$1.272 m_s T \exp \left[\frac{-22645}{T} \right] [H_2O]$
	Reverse	$1.044 \times 10^{-4} m_s T^2 \exp \left[\frac{-6319}{T} - 17.29 \right] [H_2][CO]$
CO ₂ gasification $C + CO_2 \leftrightarrow 2CO$	Forward	$1.272 m_s T \exp \left[\frac{-22645}{T} \right] [CO_2]$
	Reverse	$1.044 \times 10^{-4} m_s T^2 \exp \left[\frac{-2363}{T} - 20.92 \right] [CO]^2$
Methanation $0.5C + H_2 \leftrightarrow 0.5CH_4$	Forward	$1.368 \times 10^{-3} m_s T \exp \left[\frac{-8078}{T} - 7.087 \right] [H_2]$
	Reverse	$0.151 m_s T^{0.5} \exp \left[\frac{-13578}{T} - 0.372 \right] [CH_4]^{0.5}$
Water-Gas shift $H_2O + CO \leftrightarrow H_2 + CO_2$	Forward	$7.68 \times 10^{10} m_s T \exp \left[\frac{-36640}{T} \right] [CO]^{0.5} [H_2O]$
	Reverse	$6.4 \times 10^9 m_s T \exp \left[\frac{-39260}{T} \right] [H_2]^{0.5} [CO_2]$
Methane reforming $CH_4 + H_2O \leftrightarrow CO + 3H_2$	Forward	$3.0 \times 10^5 T \exp \left[\frac{-15042}{T} \right] [CH_4][H_2O]$
	Reverse	$0.0265 T \exp \left[\frac{-32900}{T} \right] [CO][H_2]^2$

3 Results and discussion

A number of researchers have analyzed the effect of steam to biomass ratio and carried out CFD simulations related to biomass gasification. Wei, Xu et al. 2007 has carried out experiments in a free fall reactor and used S/B ratios from 0 to 1.00 in the same temperature ranges adopted in this work. Rapagnà, Jand et al. 2000 has looked into steam gasification in a bubbling fluidized bed reactor with olivine catalysts where S/B ratio between 0.4 to 1.00 had been analyzed. Campoy, Gómez-Barea et al. 2009 has used a mixture of oxygen and steam as the gasifying agent and carried out experiments in a fluidized bed reactor without external heating of the bed. The S/B ratio was between 0 and 0.58. The simulations in this work was initiated with S/B ratio of 0.45 and bed temperature of 1023 K.

3.1 Simulation with S/B ratio of 0.45

A reduction of bed mass from 178.3 kg to 177.1 kg and char fraction of the bed outflow from 3.25% to 0.6% were observed during the simulation time of 100s. However, bed particle outflow and bed particle inflow were connected with 95% mass efficiency (assuming 5% of char availability in the bed particle outflow). The incorrect match of mass flowrate of particle flows might

lead to reduction of the bed mass. On the other hand, there is a considerable reduction of char in the bed outflow. This might be due to insufficient biomass supply compared to char outflow.

Bed hydrodynamics, temperature distribution of particles in the bed and distribution of different particle species are illustrated respectively in (a), (b) and (c) of Figure 3. Referring to the same figure, the bubbling fluidization of the reactor is clearly depicted. However, the particle temperature shows uneven characteristics, especially along the cross section. Heated particles from the combustion reactor seem to be accumulated in the opposite half to the particle inlet of the reactor. Homogeneous distribution of three particle species is illustrated Figure 3 (c) where 1, 2 and 3 in the figure are referred to sand, char and biomass respectively.

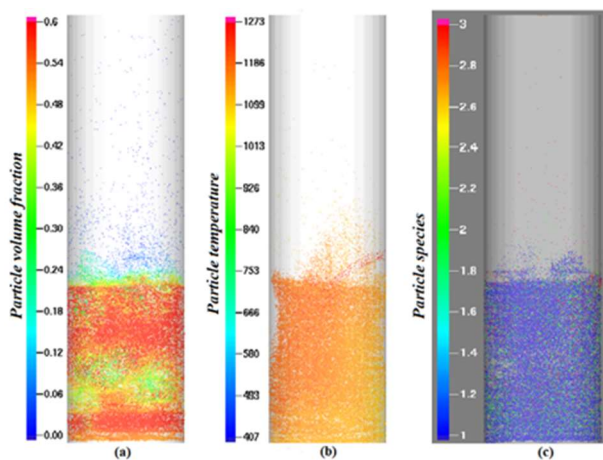


Figure 3. (a) Bubbling fluidization, (b) temperature of bed particles, (c) distribution of particle species

Product gas composition was observed in both axial and radial directions of the reactor, which are illustrated in Figure 4 and Figure 5. The final gas composition from the reactor was read from the center cell of the outflow pressure boundary, which actually acts as a sensor installed.

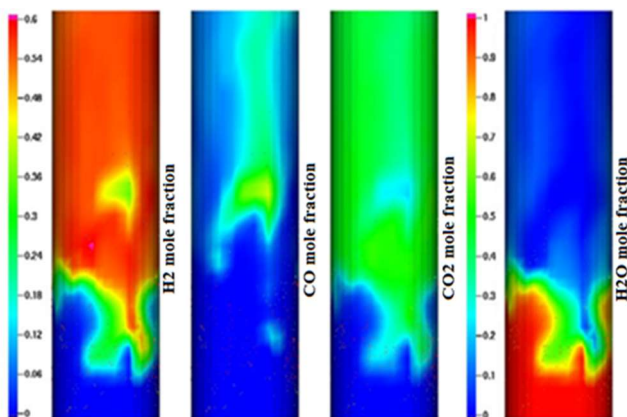


Figure 4. Product gas composition along the reactor height

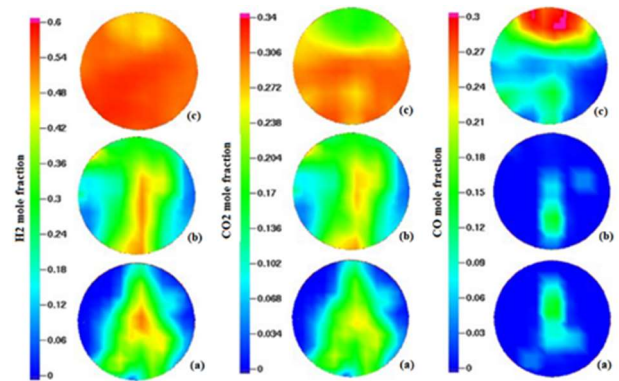


Figure 5. Gas composition at different cross sections along reactor height. (a), (b) and (c) refers to 0.3, 0.6 and 0.9m heights from the bottom of the reactor

No significant change in the gas composition is observed up to the biomass feeding point. This depicts the slow reaction kinetics of the char-steam heterogeneous reactions. The gas phase composition starts to change from the biomass feeding point, which is mainly due to pyrolysis reactions. Even though pyrolysis gas contains nearly 68% of CO, higher concentration cannot be observed even at the biomass feeding point. This is mainly due to high reaction rate of the water-gas shift reaction compared to the pyrolysis reaction, which consumes CO immediately to produce CO₂ and H₂. Therefore, H₂ and CO₂ increase along the reactor height with simultaneous decrease of CO and H₂O.

The gas production rate is also monitored, and the volumetric and mass gas production rates were approximately 0.33m³/s and 0.055kg/s respectively. The flow rates as function of time are plotted in Figure 6. Following the ideal gas law (high temperature and low pressure), the gas production rate was calculated as 1.64 Nm³/kg of biomass, which is well within the data published in literature. The area specific gas production rate, which is one of the useful parameters in reactor sizing, was observed as 0.34Nm³/s·m².

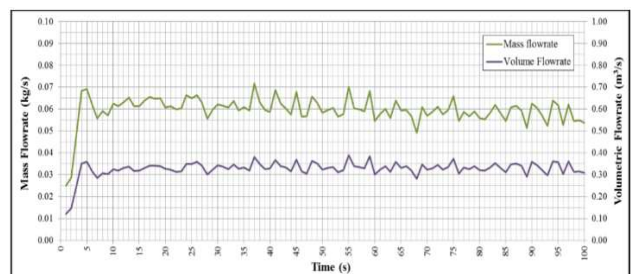


Figure 6. Time evolution product gas flowrates

The average molar gas composition during the final 25s was observed as 0.128-CO, 0.273-CO₂, 0.574-H₂ and 0.025-H₂O. The product gas heating value was calculated to be 10.1 MJ/kg where the lower heating values (LHV) of wood, CO and H₂ were taken as 16 MJ/kg (dry basis), 10 MJ/kg and 120 MJ/kg

respectively. The cold gas efficiency (CGE) was calculated as 73.3% using the equation:

$$CGE = \frac{mass_{gas}(kg)}{mass_{fuel}(kg)} \frac{LHV_{gas}(J/kg)}{LHV_{fuel}(J/kg)} \quad (2)$$

There is an uncertainty related to the calculation of cold gas efficiency because the actual operating conditions of the combustion reactor is not known. A guessed value of 200°C was taken for the temperature increment in the combustion reactor. However, there can be additional fuel supply into the combustion reactor to achieve the desired temperature rise, which indirectly affects for the cold gas efficiency.

3.2 Effect of Steam-to-Biomass ratio

The biomass flowrate was increased from 0.05kg/s to 0.06kg/s, 0.08kg/s and 0.11kg/s to adjust the S/B ratio from 0.45 to 0.38, 0.28 and 0.2 respectively. Temperatures and steam inlet flow velocity were kept unchanged. Similar characteristics of bed hydrodynamics, temperature and particle species distribution were observed as in the case with of S/B of 0.45. Figure 7 illustrates the final gas composition for the respective cases.

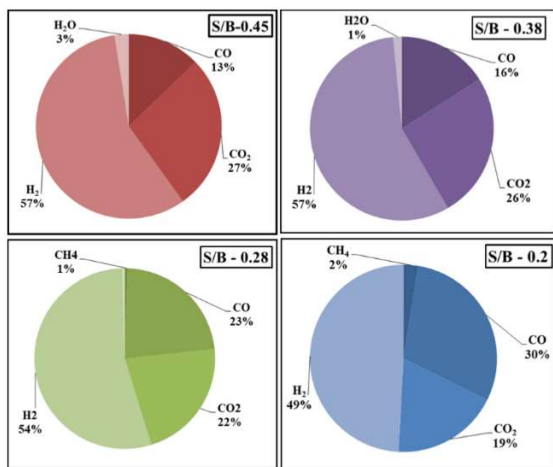


Figure 7. Molar composition of product gas

The molar concentration of H₂ is dramatically reduced from 57% at S/B of 0.45 to 49% at S/B of 0.2 showing a reduction of 8%. In contrast, the concentration of CO has increased by 17% within the respective range. According to the data presented in Figure 3-5, steam is almost totally consumed even for S/B of 0.45. However, the pyrolysis gas volumes in the successive cases of low S/B ratios is increased due to increasing biomass flowrates. As a result, low S/B operation experiences a deficiency of steam to perform the water-gas-shift reaction. Therefore, Product gas is consisted with a substantial share of raw pyrolysis gas. The unreacted fraction of the pyrolysis gas is the root cause for increasing CO concentrations in the product

gas at low S/B. This phenomenon is illustrated Figure 8. Steam reforming reaction adds mass to the pyrolysis gas, which is clear from the figure as product gas mass flowrate always runs above the pyrolysis gas curve. However, the gap between two curves gets narrowed at lower S/B. Further, two curves stand almost parallel to each other at lower S/B than approximately 0.3. The total consumption of steam at S/B of 0.3 is the reason for this behavior.

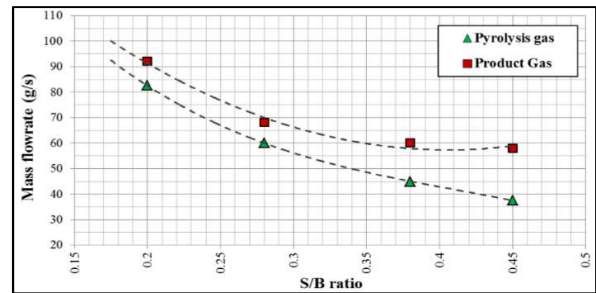


Figure 8. Pyrolysis and product gas mass flowrates

Further, noticeable amount of CH₄ is available in the product gas in both the case of 0.28 and 0.2 S/B. It is evident from the reaction kinetic data in Table 2 that the reaction rate of the water-gas-shift reaction is much higher than the methane reforming. Therefore, steam is initially consumed by CO and when it comes to the respective cases, no steam is left for methane reforming reactions.

As illustrated in Figure 9, the product gas temperature has dropped down by 50K at reduced S/B of 0.28 and 0.2. This happens as more energy is extracted for the pyrolysis reactions with increased biomass feed rate at lower S/B ratios.

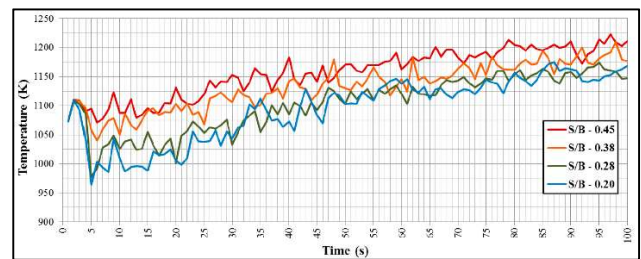


Figure 9. Time evolution product gas temperature at different S/B

The summary of other parameters at different S/B is given in Table 3. The volumetric gas production rate at S/B 0.2 has increased by 33% compared to S/B 0.45. Therefore, the gas production capacity can be increased in the same reactor, simply by changing the S/B ratio. The increase of the molar percentage of the total combustible gases (H₂+CO) in the product gas from 70% to 79% is the reason behind the increased calorific value by 22% from 10.1 MJ/kg to 12.37 MJ/kg in the respective cases. The reduction of the volumetric gas production per kg of biomass is because of the inadequate steam availability to react with the additional released pyrolysis gas at lower S/B.

Table 3. Simulation results for different S/B

	S/B-0.45	S/B-0.38	S/B-0.28	S/B-0.2
Steam flow (kg/s)	22.8	22.8	22.8	22.8
Biomass flow (g/s)	50	60	80	110
Product gas				
Mass flowrate (g/s)	58	60	68	92
Volume flowrate (m ³ /s)	0.331	0.34	0.36	0.44
Mole flowrate (mol/s)	3.36	3.5	3.9	5.1
LHV (MJ/kg)	10.1	10.54	11.5	12.37
Cold gas efficiency	73.2	65.8	61.1	64.6

4 Conclusion

Barracuda VR commercial package with the MP-PIC CFD principle, was used in this work. The product gas quality was observed at different steam-to-biomass ratios. The product gas composition, gas flowrates, heating value and cold gas efficiency showed a significant sensitivity regarding the S/B ratio and following conclusions could be made. As the steam-to-biomass ratio is reduced,

- H₂ content is decreased while CO is increased
- LHV is increased while cold gas efficiency is decreased
- Gas production rate per kg of biomass is reduced

Simulating complete dual fluidized bed reactor system together with a detailed characterization of biomass such as composition and pyrolysis kinetics, will overcome the uncertainties related to this work for a certain extent. Barracuda VR is a sophisticated tool for optimization of the effect of different parameters on the biomass gasification.

Acknowledgements

The authors would like to forward their gratitude to University College of Southeast Norway for providing of the Barracuda VR software package and computer facilities.

References

Andrews, M. J. and P. J. O'Rourke (1996). "The multiphase particle-in-cell (MP-PIC) method for dense particulate flows." *International Journal of Multiphase Flow* **22**(2): 379-402.

Bandara, J. C., R. K. Thapa, B. M. E. Moldestad and M. S. Eikeland (2016). "Simulation of Particle Segregation in Fluidized Beds." *9th EUROSIM Congress on Modelling and Simulation*, Oulu, Finland, IEEE.

Campoy, M., A. Gómez-Barea, F. B. Vidal and P. Ollero (2009). "Air-steam gasification of biomass in a fluidised bed: Process optimisation by enriched air." *Fuel Processing Technology* **90**(5): 677-685.

Century, R. E. P. N. f. t. s. (2015). "RENEWABLES 2015 - Global Status Report", Paris: REN21 Secretariat.

Demirbas, A. (2008). "Biofuels sources, biofuel policy, biofuel economy and global biofuel projections." *Energy Conversion and Management* **49**(8): 2106-2116.

Liang, Y., Y. Zhang, T. Li and C. Lu (2014). "A critical validation study on CPFD model in simulating gas-solid bubbling fluidized beds." *Powder Technology* **263**: 121-134.

Liu, H., R. J. Cattolica and R. Seiser (2016). "CFD studies on biomass gasification in a pilot-scale dual fluidized-bed system." *International Journal of Hydrogen Energy* **41**(28): 11974-11989.

Liu, H., R. J. Cattolica, R. Seiser and C.-h. Liao (2015). "Three-dimensional full-loop simulation of a dual fluidized-bed biomass gasifier." *Applied Energy* **160**: 489-501.

Loha, C., H. Chattopadhyay and P. K. Chatterjee (2014). "Three dimensional kinetic modeling of fluidized bed biomass gasification." *Chemical Engineering Science* **109**: 53-64.

Munasinghe, P. C. and S. K. Khanal (2010). "Biomass-derived syngas fermentation into biofuels: Opportunities and challenges." *Biorescience Technology* **101**(13): 5013-5022.

Naik, S. N., V. V. Goud, P. K. Rout and A. K. Dalai (2010). "Production of first and second generation biofuels: A comprehensive review." *Renewable and Sustainable Energy Reviews* **14**(2): 578-597.

R.K. Thapa, C. Pfeifer and B. M. Halvorsen (2014). "Modeling of reaction kinetics in bubbling fluidized bed biomass gasification reactor" *INTERNATIONAL JOURNAL OF ENERGY AND ENVIRONMENT* **5**(1): 10.

Rapagnà, S., N. Jand, A. Kiennemann and P. U. Foscolo (2000). "Steam-gasification of biomass in a fluidised-bed of olivine particles." *Biomass and Bioenergy* **19**(3): 187-197.

Scarlat, N., J.-F. Dallemand, O. J. Skjelhaugen, D. Asplund and L. Nesheim (2011). "An overview of the biomass resource potential of Norway for bioenergy use." *Renewable and Sustainable Energy Reviews* **15**(7): 3388-3398.

Snider, D. M. (2001). "An Incompressible Three-Dimensional Multiphase Particle-in-Cell Model for Dense Particle Flows." *Journal of Computational Physics* **170**(2): 523-549.

Snider, D. M., S. M. Clark and P. J. O'Rourke (2011). "Eulerian-Lagrangian method for three-dimensional thermal reacting flow with application to coal gasifiers." *Chemical Engineering Science* **66**(6): 1285-1295.

Solnordal, C. B., V. Kenche, T. D. Hadley, Y. Feng, P. J. Witt and K. S. Lim (2015). "Simulation of an internally circulating fluidized bed using a multiphase particle-in-cell method." *Powder Technology* **274**: 123-134.

Szczodrak, J. and J. Fiedurek (1996). "Technology for conversion of lignocellulosic biomass to ethanol." *Biomass and Bioenergy* **10**(5): 367-375.

Wei, L., S. Xu, L. Zhang, C. Liu, H. Zhu and S. Liu (2007). "Steam gasification of biomass for hydrogen-rich gas in a free-fall reactor." *International Journal of Hydrogen Energy* **32**(1): 24-31.

Xie, J., W. Zhong, B. Jin, Y. Shao and H. Liu (2012). "Simulation on gasification of forestry residues in fluidized beds by Eulerian-Lagrangian approach." *Biorescience Technology* **121**: 36-46.